Available online at www.sciencedirect.com
ScienceDirect
Biochimica et Biophysica Acta 1777 (2008) 118–129
Biochimica et Biophysica Acta
BBA
www.elsevier.com/locate/bbabio

Uncoupling protein-2 accumulates rapidly in the inner mitochondrial membrane during mitochondrial reactive oxygen stress in macrophages

Tindaro M. Giardina, James H. Steer, Susan Z.Y. Lo, David A. Joyce *

Pharmacology Unit, School of Medicine and Pharmacology, University of Western Australia, 35 Stirling Highway, Crawley, Western Australia 6009, Australia

Received 31 May 2007; received in revised form 9 November 2007; accepted 12 November 2007
Available online 22 November 2007

Abstract

Uncoupling protein-2 (UCP2) is a member of the inner mitochondrial membrane anion-carrier superfamily. Although mRNA for UCP2 is widely expressed, protein expression is detected in only a few cell types, including macrophages. UCP2 functions by an incompletely defined mechanism, to reduce reactive oxygen species production during mitochondrial electron transport. We observed that the abundance of UCP2 in macrophages increased rapidly in response to treatments (rotenone, antimycin A and diethyldithiocarbamate) that increased mitochondrial superoxide production, but not in response to superoxide produced outside the mitochondria or in response to H_2O_2. Increased UCP2 protein was not accompanied by increases in *ucp2* gene expression or mRNA abundance, but was due to enhanced translational efficiency and possibly stabilization of UCP2 protein in the inner mitochondrial membrane. This was not dependent on mitochondrial membrane potential. These findings extend our understanding of the homeostatic function of UCP2 in regulating mitochondrial reactive oxygen production by identifying a feedback loop that senses mitochondrial reactive oxygen production and increases inner mitochondrial membrane UCP2 abundance and activity. Reactive oxygen species-induction of UCP2 may facilitate survival of macrophages and retention of function in widely variable tissue environments.

Keywords: Uncoupling protein-2; Macrophage; Superoxide; Reactive oxygen species; Mitochondria

1. Introduction

Uncoupling proteins belong to the superfamily of inner mitochondrial membrane anion-carrier proteins that also includes the adenine nucleotide translocases (ANT's) and the phosphate, oxoglutarate/malate, carnitine, citrate, ornithine and dicarboxylate carriers [1]. The first described uncoupling protein family member, uncoupling protein-1 (UCP1) [2,3], is expressed solely in the inner mitochondrial membrane of brown adipose tissue at sufficiently high levels to be responsible for thermogenesis [4,5]. Uncoupling protein-2 (UCP2) is expressed widely in tissues and cell types [6,7] but in amounts too low to be involved in thermoregulation [6,8–10].

UCP2 is best characterized as a regulator of reactive oxygen species during electron transport in the mitochondrial inner membrane. During normal mitochondrial respiration, a proportion of electrons transferring between coenzyme Q and complex I or complex III divert to reducing molecular oxygen to superoxide ($O_2^{\bullet -}$). Further steps of reduction can yield hydrogen peroxide and the highly reactive hydroxyl radical [11]. Interaction between reactive oxygen species and biological molecules can then generate a range of nitrogen- and carbon-centred radical species and modified proteins and lipids. Systems of low molecular weight reductants, sulfhydryl-containing protein re-

Abbreviations: UCP2, Uncoupling protein-2; ANT, adenine nucleotide translocase; UCP1, uncoupling protein-1; $O_2^{\bullet -}$, superoxide; $\Delta\psi_m$, mitochondrial membrane potential; TIM, transporter of inner mitochondrial membrane; DMEM, Dulbecco's Modified Eagle Medium; FCS, foetal calf serum; BMM, murine bone marrow-derived monocyte/macrophages; ROS, reactive oxygen species; HBSS, Hanks balanced salt solution; DETC, diethyldithiocarbamate; JC-1, 5,5′,6,6′-tetrachloro-1,1′,3,3′-tetraethylbenzimidazol carbocyanine iodide; CCCP, carbonyl cyanide *m*-chlorophenylhydrazone: 6-carboxy-H_2DCF-DA-AM, 6-carboxy-2′,7′-dichlorodihydrofluorescein diacetate, di (acetoxymethyl ester); DHE, dihydroethidium; Et, ethidium; DMNQ, 2, 3-dimethoxy-1, 4-naphthoquinone

* Corresponding author. Tel.: +61 8 9346 2569; fax.: +61 8 9346 3469.
E-mail address: david.joyce@uwa.edu.au (D.A. Joyce).

0005-2728/$ - see front matter © 2007 Elsevier B.V. All rights reserved.
doi:10.1016/j.bbabio.2007.11.006

ductants, superoxide dismutases and peroxidases act in mitochondria to detoxify reactive oxygen species.

Increased electron "leakage" to $O_2^{\bullet-}$ production occurs when electron transfer is slowed at complexes I and III [12–16], either through the action of inhibitors at these sites (such as rotenone and antimycin A, respectively) or because of elevated mitochondrial membrane potential ($\Delta\psi_m$). The $\Delta\psi_m$ reflects the pumping of protons from the matrix side of the inner mitochondrial membrane to the intermembrane side at complexes I, III and IV. The backflow of protons through F_0/F_1 ATPase generates ATP, a process that is normally in tight energetic coupling with electron transport. Mitochondrial $O_2^{\bullet-}$ production is non-linearly increased when proton pumping forces $\Delta\psi_m$ more negative than approximately −150mV [12,13,17]. Under these circumstances, mild uncoupling of the electron transport chain of the inner mitochondrial membrane dramatically reduces $O_2^{\bullet-}$ production [18,19].

The primary function of the brown fat uncoupling protein, UCP1, is to provide a proton channel that returns protons to the mitochondrial matrix, so oxidative metabolism yields heat, rather than ATP. In-vitro, UCP2 likewise serves to dissipate transmembrane proton gradients, though the exact mechanism is incompletely defined. UCP2 expression in the inner mitochondrial membrane lowers mitochondrial $O_2^{\bullet-}$ production, consistent with a mild uncoupling function [20]. Increased mitochondrial reactive oxygen species production thus occurs in macrophages of homozygous *ucp2* gene-deleted mice [8]. Conversely, tissue-specific overexpression of UCP2 in pancreatic beta islet cells lowers mitochondrial reactive oxygen production [21]. Isolated cells of various lineages have shown similar results [18,22,23].

UCP2 regulation of reactive oxygen species in macrophages is notable. Macrophages exist as resident or inflammatory populations in environments with widely varying nutrient availability and oxygenation. Resident alveolar macrophages experience O_2 tensions exceeding other tissues, whereas tumor-associated macrophages remain functional at the low O_2 tensions that characterize hypoxic areas of tumor [24–26]. There is a corresponding variation in dependence on oxidative phosphorylation and, it follows, different potential for mitochondrial reactive oxygen species generation [27]. Alternate aerobic energy sources include glucose, glutamine and fatty acids. Under hypoxic conditions, anaerobic glycolysis supplies ATP requirements [24,28]. Macrophages at sites of chronic inflammation are also exposed to reactive oxygen species produced at the surface NADPH oxidases of activated cells of the myelomonocytic lineage, including macrophages themselves [29].

It is therefore reasonable to inquire whether macrophages have a particular need for flexible regulation of $\Delta\psi_m$, so as to keep mitochondrial reactive oxygen species production within physiological bounds. This could be achieved if UCP2 activity or abundance varied in reaction to mitochondrial reactive oxygen species production. Functionally, $O_2^{\bullet-}$ and reactive oxygen species-derived products of lipid peroxidation, such as 4-hydroxynonenal do promote UCP2 uncoupling activity in isolated membrane preparations [16,18,30,31]. There is now also evidence that UCP2 abundance may vary in response to oxidative stress: an increase of 12-fold in UCP2 protein expression in murine lung after exposure to gram-negative bacterial lipopolysaccharide was attributed to oxidative stress [6].

ucp2 is encoded in the nuclear genome. Transcriptional regulation has been described and extensively studied, but it is clear that post-transcriptional events also strongly influence protein abundance [32]. For example, the increase in pulmonary UCP2 protein that followed lipopolysaccharide exposure was not accompanied by an increase in mRNA expression [6]. Early studies of UCP2 message levels in tissues have also proved poorly predictive of protein expression [7,33]. Importation of UCP2 into mitochondrial inner membrane and degradation are also potentially regulable processes. Little is known about these. UCP2 lacks identified mitochondrial targeting sequences and has not yet been shown to be a substrate for the transporter of inner mitochondrial membrane (TIM) proteins.

Evidence for UCP2 regulation in response to oxidative stress in lung, coupled with evidence that UCP2 diminishes mitochondrial production of oxidizing radicals in macrophages [8,23] suggests that macrophages might regulate expression of UCP2 to cope with changes in nutrient availability, oxygenation and oxidative stress in their environment. We therefore measured the effects of mitochondrial oxidative stress on the expression of UCP2 and explored the mechanism of regulation.

2. Materials and methods

2.1. Cell lines and reagents

The murine macrophage cell line, $RAW_{264.7}$, was obtained from American Type Culture Collection (ATCC). Cells were maintained in Dulbecco's Modified Eagle Medium (DMEM) (Life Technologies, Melbourne, Australia) supplemented with 5% low endotoxin foetal calf serum (FCS) (CSL, Melbourne, Australia), penicillin and gentamicin (DMEM/FCS). Cells were incubated in DMEM/FCS in a humidified atmosphere of 5% CO_2/95% air at 37 °C. Primary murine bone marrow-derived monocyte/macrophages (BMM) were isolated from long bones of C57/BL mice, as previously described [34], and expanded in 25cm^2 culture flasks for 7days in DMEM/FCS supplemented with 50ng/ml of human macrophage-colony stimulating factor (R&D Systems). The medium was replaced on the 4th day. Cells were then treated as for $RAW_{264.7}$ cells.

Reagents were supplied by Sigma, except where indicated.

2.2. Cell fractionation and protein analyses

$RAW_{264.7}$ cells at 80% confluence in 25cm^2 flasks were exposed to rotenone (10μM), the Cu/Zn superoxide dismutase inhibitor, diethyldithiocarbamate (DETC: 0.3mM), antimycin A (10 μM), the site III inhibitor myxothiazole (10μM) or the cytosolic redox-cycling agent, 2,3-dimethoxy-1,4-naphthoquinone (DMNQ: 10μM). After incubation, medium was removed and cultures were placed on ice and washed with ice-cold Dulbecco's Phosphate Buffered Saline. Whole cell extracts were made in RIPA buffer containing Complete Protease Inhibitors (Roche). Cells for mitochondrial fractionation were scraped into ice-cold TES buffer (10mM Tris, 1mM EDTA, 250mM sucrose pH 7.5) containing protease inhibitors. Cells were collected by centrifugation and then sequentially homogenized in ice-cold TES buffer using a Dounce homogenizer and passed through a 30g needle. The homogenate was centrifuged at 750*g* for 10min at 4 °C. The resulting supernatant was centrifuged again at 11,000*g* for 30min at 4 °C to obtain the mitochondria-enriched pellet. The mitochondrial pellet was washed in cold TES buffer and re-centrifuged, to remove contamination of membrane fractions. The final pellet was resuspended in RIPA buffer containing protease inhibitors and stored at −20 °C. Inclusion of EDTA in buffers limits the binding of polysomes, which may be in association with nascent UCP2, to mitochondria [35].

To obtain mitoplasts and a fraction enriched in intermembrane space proteins, the mitochondrial fractions were incubated with digitonin (0.4mg/mg of mitochondrial protein) and TES buffer on ice for 15min [36]. The mitoplast and membrane fraction was separated from the fraction containing the intermembrane space proteins by centrifugation at 11,000*g* for 15min at 4 °C. The mitoplast pellet was washed in TES buffer and centrifuged once again. The final mitoplast pellet was lysed in RIPA buffer containing Roche Complete Protease Inhibitor and stored at−20 °C. The supernatant was transferred to a Beckman 1.5ml Polyallomer Microfuge® Tube and centrifuged at 100,000*g* for 40min at 4 °C in a TL-100 ultracentrifuge (Beckman) equipped with a TLA45 rotor, to sediment remaining membrane material. The supernatant containing the intermembrane fraction was removed and stored at −20 °C.

Whole cell and mitochondrial fraction extracts (30–100μg total protein) were separated by SDS-10% polyacrylamide gel electrophoresis, transferred onto PVDF membrane and probed with specific antibodies to UCP2 (Santa Cruz Biotechnology, Santa Cruz, CA; sc-6526) and β-actin (Sigma, St. Louis, MO; A-5441). A goat anti-UCP2 polyclonal antibody (sc-6526; 1:1000 dilution), followed by anti-goat HRP IgG (Santa Cruz, sc-2020; 1:10,000) was used to detect UCP2. β-actin was detected using a mouse monoclonal anti-β-actin antibody (Sigma, A-5441; 1:10,000 dilution), followed by anti-mouse HRP IgG antibody (Sigma, A-2554); 1:10,000). Porin1 (VDAC1) was detected using a goat antibody (Santa Cruz, 8828; 1:1000 dilution), followed by anti-goat HRP IgG antibody (Santa Cruz, sc-2020; 1:5000). The resolved bands were visualized by enhanced chemiluminescence (ECL) detection reagents (Amersham) and exposed to Hyperfilm ECL (Amersham) for 0.5–5min. Densitometric quantitation of X-ray film was performed using Kodak Molecular Imaging Software, Version 4.0 (Kodak). Statistical analysis of treatment effects on UCP2 expression employed data that was normalised for β-actin expression.

The specificity of the anti-UCP2 antibody was confirmed by transiently expressing UCP2 in HEK 293 cells to generate a verified standard. To create the expression vector for UCP2, the coding region was amplified from rat cDNA using the primers (sense) 5′-GGTACCATGGTTGGTTTCAAGGCCACCGATGTGCC-3′ and (antisense) 5′-GAGCTCAGTTTTCCCCACGGAGGGCCCTAAGTAT-3′. The restriction sites *Kpn*1 and *Xho*1 (underlined) were used for ligation (LigaFast ligation system [Promega]) into the multiple cloning region of pcDNA3.1 (Invitrogen). The vector was confirmed by sequencing. Rat UCP2 differs from murine UCP2 by two conservative amino acid substitutions. HEK 293 cells transiently transfected with the parent vector did not contain a protein that was detectable with the antibody (Fig. 3A).

2.3. Transcription studies

To examine the regulation of UCP2 gene transcription, a fragment corresponding to bases − 2746 to +100 of the UCP2 gene (Pubmed accession NM_011671) was amplified from murine genomic DNA using the primers (sense) 5′-CGCGGTACCACACACTAGCCTCCAGGACC-3′ and (antisense) 5′-ATGAACGCGTGAGAACACAGGAGTGCAGAA-3′. The underlined sequences indicate *Kpn*I and *Mlu*I sites required for cloning into the expression system. The fragment was ligated into the multiple cloning site of the pGL_3-basic luciferase expression vector (Promega). The vectors were verified by sequencing. The pGL_3-basic vector was used as control.

For transient transfection, adherent $RAW_{264.7}$ cells (approximately 10^7) were released by trypsin exposure, pelleted in DMEM/FCS by centrifuging at 300*g* for 5min, and resuspended in 750μl of antibiotic-free RPMI (Life Technologies) containing 20mM HEPES pH 7.4. Cells were then transfected according to a DEAE-Dextran protocol, as previously described [37]. Transfected $RAW_{264.7}$ cells were then transferred to 24 well cell culture plates (3.3×10^5cells/well) and rested overnight before being exposed to the indicated agents. Cell lysates were prepared and firefly luciferase expression was measured using the Promega Luciferase Assay System, according to manufacturer's instructions.

2.4. mRNA analysis

$RAW_{264.7}$ cells and primary macrophages (0.8×10^5 per well) were cultured for 48h in 6 well cell culture plates before exposure to rotenone, antimycin A or DETC. Total cellular RNA was isolated using RNeasy® Protect Mini Kit (Qiagen) in accordance with the manufacturer's protocol. The Omniscript Reverse Transcriptase Kit (Qiagen) was used to for first-strand cDNA synthesis. PCR reactions were completed using an iCycler iQ Multi-Color Real-Time PCR Detection System (Bio-Rad) and SYBR Green PCR MasterMix (Bio-Rad) containing the SYBR green fluorescent reporter and Taq polymerase for cDNA amplification. Aliquots of sample cDNAs were used to create separate standard curves for relative quantification of UCP2 and β-actin genes. Sample cDNAs (equivalent of 5ng of total RNA) were amplified by target specific primers for UCP2; (sense) 5′-GGGTCCACGCAGCCTCTACAATG-3′, (antisense) 5′-TCCCTTCCTCTCGTGCAATGGTCT-3′ and β-actin; (sense) 5′-CCTGACGGACTACCTCATGAA-3′, (antisense) 5′-GATGCCACAGGATTCCATA-3′. The specificity of individual primers was tested by end point PCR and validated by detection through gel electrophoresis. Thermal profiles for the amplification were: 95 °C for 3min, then 40 cycles of 95 °C for 10s and 58 °C for 30s. A melt temperature gradient curve was also carried out on final reaction products to ensure that a single product had formed. Each sample was normalized using its β-actin content as internal reference, and data are expressed as relative abundance of UCP2 mRNA over β-actin mRNA.

2.5. Mitochondrial membrane potential

$RAW_{264.7}$ cells were seeded ($2–5\times10^4$ per well) in DMEM/FCS in clear 96-well plates (Nunc) and after 42–48h loaded with 1μg/ml 5,5′,6,6′-tetrachloro-1,1′,3,3′-tetraethylbenzimidazol carbocyanine iodide (JC-1) in DMEM/FCS for 20min. JC-1 is a cationic cell-permanent dye that exhibits potential-dependent accumulation in mitochondria. Mitochondrial membrane potential was estimated from the ratio of red (590nm) to green (520nm) emission fluorescence (green denoting a more depolarized state and red a more polarized state) under 485nm excitation, using a fluorescence microplate reader (POLARstar OPTIMA, BMG, Germany). Control conditions for these experiments included exposure to the proton ionophore, carbonyl cyanide m-chlorophenylhydrazone (CCCP), which depolarises $\Delta\psi_m$ and to the F_0F_1 ATPase inhibitor oligomycin, which hyperpolarises $\Delta\psi_m$.

2.6. Fluorescent detection of mitochondrial reactive oxygen species (ROS)

Superoxide and H_2O_2 were measured in $RAW_{264.7}$ and bone marrow macrophages ($2–5\times10^4$) that had been maintained in clear 96-well plates over two days (42–48h) in DMEM/FCS. To estimate $O_2^{\bullet-}$ production, cells were loaded with dihydroethidium (DHE: 10μM; Invitrogen) for 15min in DMEM/FCS and then transferred to Hanks balanced salt solution (HBSS), where the conversion to ethidium (Et) was measured as emission at 590nm during excitation at 540nm in a POLARstar OPTIMA microplate reader over 3h at 37 °C [38,39]. H_2O_2 generation was estimated from the accumulation of 6-carboxy-DCF [38,39] in cells that had been loaded with 3μM 6-carboxy-2′,7′-dichlorodihydrofluorescein diacetate, di(acetoxymethyl ester) (6-carboxy-H_2DCF-DA-AM: Invitrogen C-2938) for 45min in HBSS before transfer to fresh HBSS for measurement. 6-carboxy-DCF was measured as 520nm emission during 485nm excitation over 3h at 37 °C.

2.7. Statistical analysis

Statistical differences between control and test groups were analysed by one-way ANOVA and a post-hoc Newman–Keuls test or paired *t*-test as indicated in the figure legends (SigmaStat, Jandel Scientific). All results presented are the mean±S.E.M.

3. Results

3.1. Inhibitors of mitochondrial complexes I and III, superoxide dismutase inhibition and cytosolic redox-cycling reagents increase reactive oxygen species in macrophages

Conversion of the probe dihydroethidium (DHE) to fluorescent ethidium (Et) was used to measure $O_2^{\bullet-}$ generation in murine macrophages. The mitochondrial electron transport

chain site I inhibitor, rotenone (10μM), and the site III inhibitor, antimycin A (10μM), increase $O_2^{\bullet-}$ production in primary murine bone-marrow derived macrophages over 90 min and in the $RAW_{264.7}$ murine macrophage line over 3h (Fig. 1A). The Cu/Zn superoxide dismutase inhibitor diethyldithiocarbamate (DETC) (0.3mM), the site III inhibitor myxothiazole (10μM) and the cytosolic redox-cycling 2,3-dimethoxy-1,4-naphthoquinone (DMNQ) (10μM) likewise increased ethidium signal (Fig. 1B). H_2O_2 production was measured in parallel $RAW_{264.7}$ cell cultures as generation of the fluorescent 6-carboxydichlorofluorescein (6-carboxy-DCF) after loading with 6-carboxy-H_2DCF-DA-AM [38,39]. H_2O_2 increased in cells exposed to rotenone, antimycin A and DMNQ, consistent with the further reduction or dismutation of the $O_2^{\bullet-}$ (Fig. 2). In the presence of DETC, 6-carboxy-DCF signal fell, in keeping with inhibited dismutation of $O_2^{\bullet-}$ to H_2O_2 (Fig. 2). These findings give confidence that the ethidium signal observed in these cells truly reflects $O_2^{\bullet-}$ generation. Added hydrogen peroxide (100μM) and glucose oxidase (10U/ml) also increased 6-carboxy-DCF signal, as expected (Fig. 2).

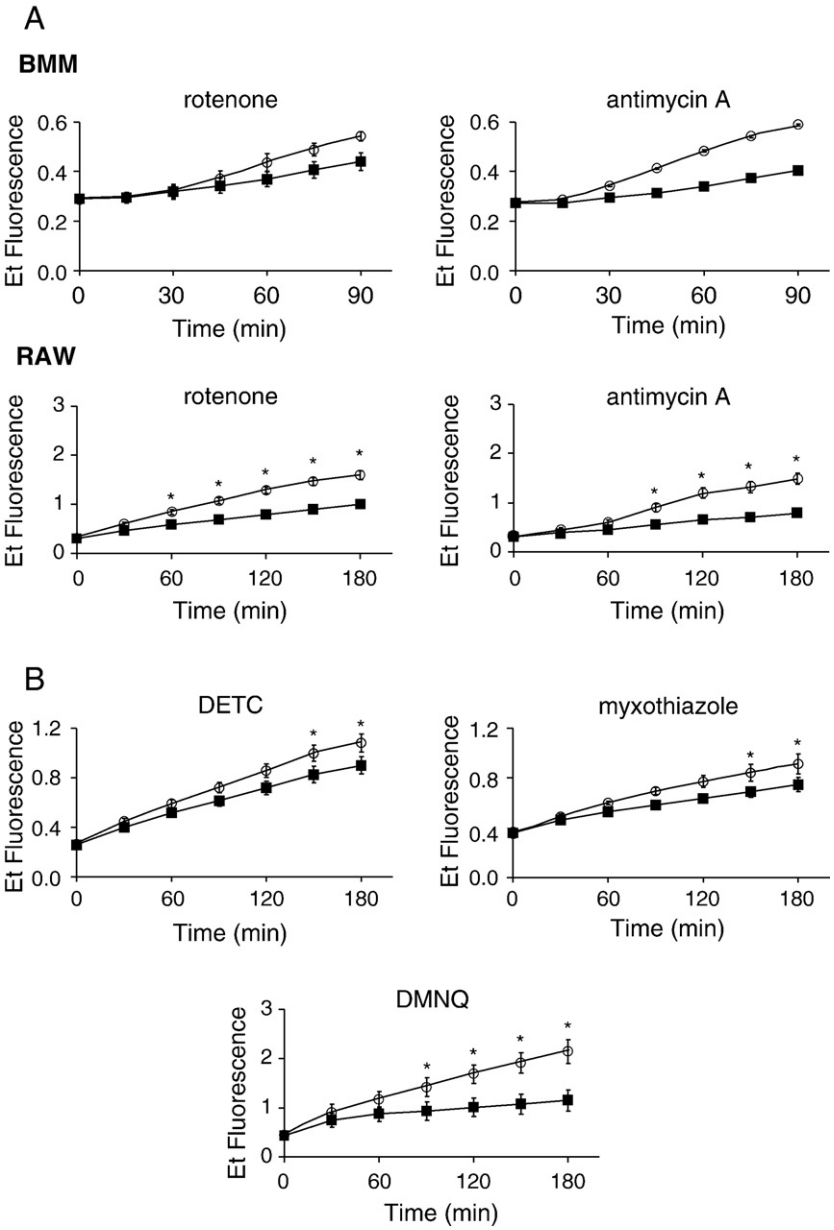

Fig. 1. Inhibitors of mitochondrial complexes I and III, DMNQ and DETC increase $O_2^{\bullet-}$ in macrophages. (A) Rotenone (10 μM) and antimycin A (10 μM) increased $O_2^{\bullet-}$ generation, as measured by ethidium fluorescence over 90 and 180 min in bone-marrow derived macrophages (BMM) and $RAW_{264.7}$ cells respectively. Data from $RAW_{264.7}$ cells are means ± S.E.M for over 25 independent experiments each for rotenone and antimycin A, *$p<0.05$ for comparison of treated and control cells. BMM data were obtained from 2 independent experiments for rotenone and 1 experiment for antimycin A. All conditions were tested in quintuplicate. –■–: control; –○–: treated with reagent named on panel. (B) The cytosolic redox-cycling agent, DMNQ (10 μM), the Cu/Zn SOD inhibitor, DETC (0.3 mM) and the site III inhibitor myxothiazole (10 μM) likewise increase ethidium signal in $RAW_{264.7}$ cells. Results are means ± S.E.M for 3 independent experiments for DMNQ and myxothiazole and 7 for DETC, each in quintuplicate. *$p<0.05$ for comparison of treated and control cells.

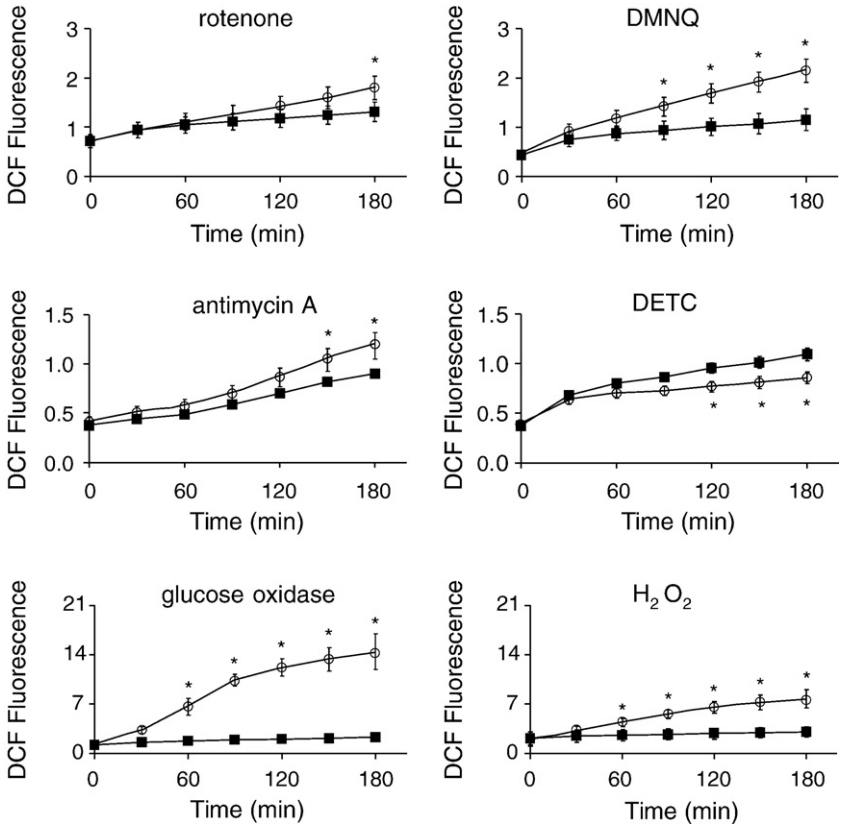

Fig. 2. Inhibitors of mitochondrial complex I and complex III and reagents that generate ROS in the cytosol increase H_2O_2 production in macrophages. Rotenone, antimycin A and DMNQ increased generation of the H_2O_2, as estimated by generation of the fluorophore 6-carboxy-DCF. H_2O_2 (100 μM) added directly or generated extracellularly by glucose oxidase (10 U/ml), also increased DCF signal. DETC inhibits dismutation of $O_2^{\bullet-}$ to H_2O_2, reducing 6-carboxy-DCF signal. Data are means ± S.E.M for $RAW_{264.7}$ macrophages of at least 7 independent experiments each for rotenone, antimycin A and DETC and 3 experiments each for DMNQ, H_2O_2 and glucose oxidase with each condition performed in quintuplicate. –■–: control; –○–: treated with reagent named on panel. Concentrations of rotenone, antimycin A, DMNQ and DETC were as in Fig. 1. *$p<0.05$ for comparison of treated and control cells.

3.2. Increased mitochondrial production of $O_2^{\bullet-}$, but not increased cytosolic $O_2^{\bullet-}$ or exogenous H_2O_2, associates with increased UCP2 protein expression

Exposure to rotenone increased UCP2 protein expression in primary murine macrophages (Fig. 3A) and $RAW_{264.7}$ cells. Increased expression was apparent by 30min and reached a peak in $RAW_{264.7}$ cells after 2 to 4h (Fig. 3B). Comparable elevations were observed in $RAW_{264.7}$ cells exposed to antimycin, DETC and myxothiazole (Fig. 3B). All these treatments increase mitochondrial $O_2^{\bullet-}$ generation (Fig. 1A and B). DMNQ, which produces $O_2^{\bullet-}$ extracellularly and in the cytosol [40] failed to increase UCP2 (Fig. 3C). LPS or TPA, both of which increase $O_2^{\bullet-}$ generation by surface NADPH oxidase also failed to alter UCP2 expression (Fig. 3C).

Glucose oxidase generates H_2O_2 continuously in the presence of glucose, without increasing mitochondrial reactive oxygen species production. Neither glucose oxidase nor bolus addition of H_2O_2 altered UCP2 expression (Fig. 3C).

We had therefore observed that increased UCP2 protein expression accompanied each of the treatments that increased mitochondrial $O_2^{\bullet-}$ production, but did not accompany treatments that increased $O_2^{\bullet-}$ or H_2O_2 generation elsewhere in the cell, or extracellularly. We therefore went on to investigate the mechanism underlying the regulation.

3.3. Increased mitochondrial $O_2^{\bullet-}$ generation is not accompanied by increased ucp2 promoter activity or an increase in UCP2 mRNA

$RAW_{264.7}$ cells were transfected with a reporter vector construct that incorporated the −2764 to +100 sequence of the UCP2 promoter upstream of the luciferase coding sequence, as described in Methods. Cells were then exposed to stimuli that increased mitochondrial $O_2^{\bullet-}$ production and luciferase activity was measured for up to 6h. None of the treatments increased *ucp2* promoter activity (Fig. 4A). At late time points, when UCP2 protein was clearly increased (Fig. 3B), rotenone-, antimycin A- and DETC-exposed cultures had lost *ucp2* promoter activity. ATP levels were comparable in treated and control cultures, indicating preserved viability over 6h (results not shown). We concluded that increased UCP2 expression was not due to any effect on *ucp2* transcription.

The effect of increased mitochondrial $O_2^{\bullet-}$ production on overall abundance of UCP2 mRNA was then examined with

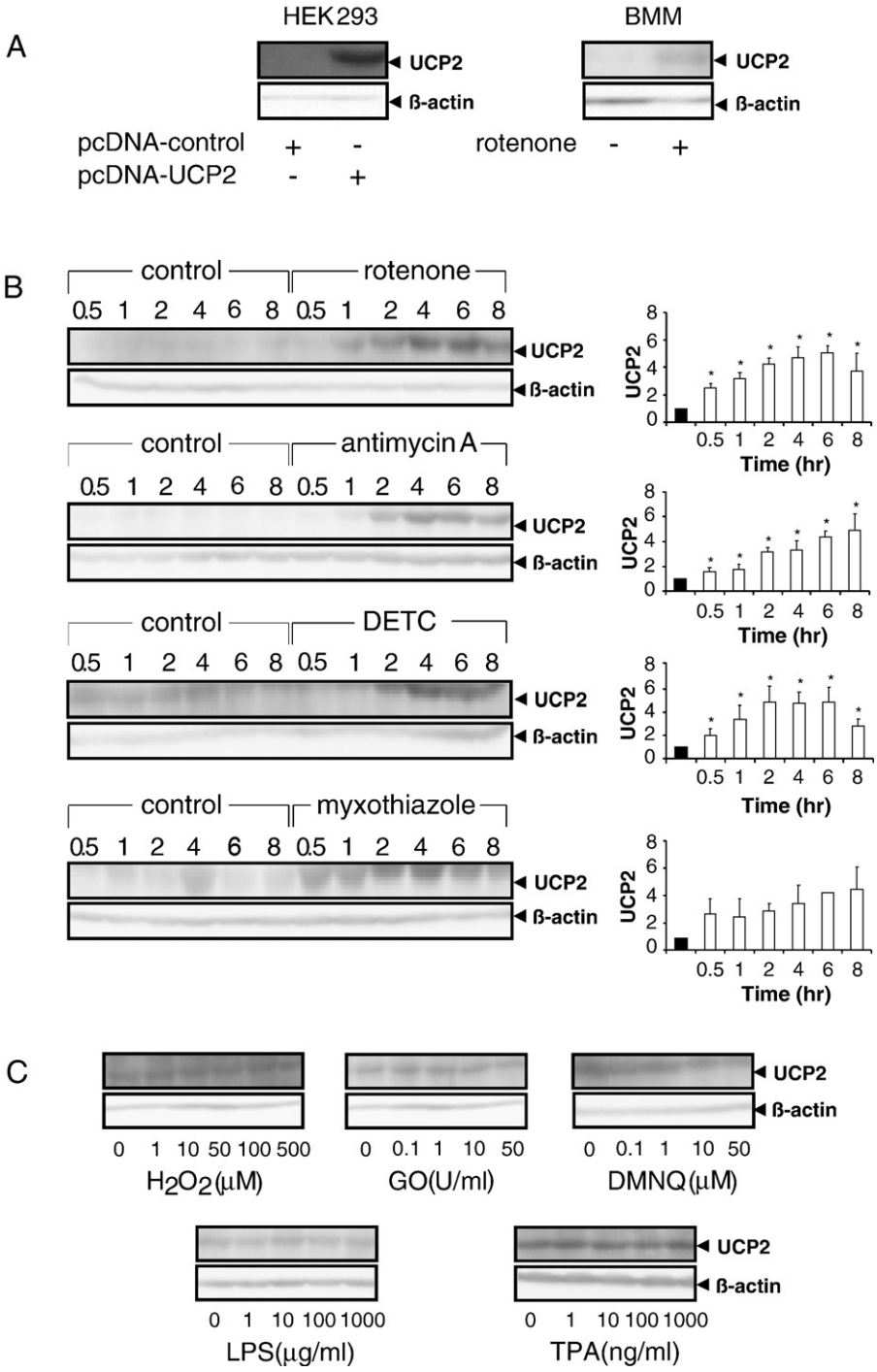

Fig. 3. Increased UCP2 protein expression follows increased mitochondrial $O_2^{\bullet-}$ production, but not $O_2^{\bullet-}$ or H_2O_2 production elsewhere in the cell or extracellularly. (A) HEK 293 cells transiently transfected with an expression vector that coded for rat UCP2 express a protein of the size of UCP2 that is recognized by a specific antibody. The same band is inducible in primary murine bone marrow-derived macrophages exposed to 10 μM rotenone for 6 h. Results are representative of 2 independent experiments in each case. (B) Rotenone, antimycin A, DETC and myxothiazole increase UCP2 expression at the same concentrations that increased $O_2^{\bullet-}$ generation in Fig. 1. Left panels show representative western analyses. Right panels show relative UCP2 band densities in western analyses of extracts from rotenone- ($n=12$), antimycin A- ($n=5$), DETC- ($n=4$) and myxothiazole- ($n=2$) treated cells, compared with controls. UCP2 density was referenced to β-actin density at each point. *$p<0.05$ for comparison of treated and control cells. (C) Reagents that increase $O_2^{\bullet-}$ generation extracellularly or elsewhere in the cell (DMNQ, LPS and TPA) and agents that increase H_2O_2 (glucose oxidase, H_2O_2) fail to increase UCP2 over 2 h, at any concentration tested. Results are representative blots of 2 independent experiments for DMNQ, H_2O_2, glucose oxidase (GO), LPS and TPA. Experiments that extended observations to 8 h with DMNQ (10 μM), H_2O_2 (100 μM), glucose oxidase (10 U/ml), LPS (10 μg/ml) and TPA (10 μg/ml) also found no increase in UCP2 (results not shown).

quantitative real-time relative RT-PCR using specific primers as described in Methods. β-actin mRNA served as the internal standard. Rotenone failed to increase the abundance of UCP2 mRNA over 6h in either primary macrophages or $RAW_{264.7}$ cells (Fig. 4B). Antimycin A and DETC similarly failed to increase UCP2 mRNA in $RAW_{264.7}$ cells (Fig. 4B).

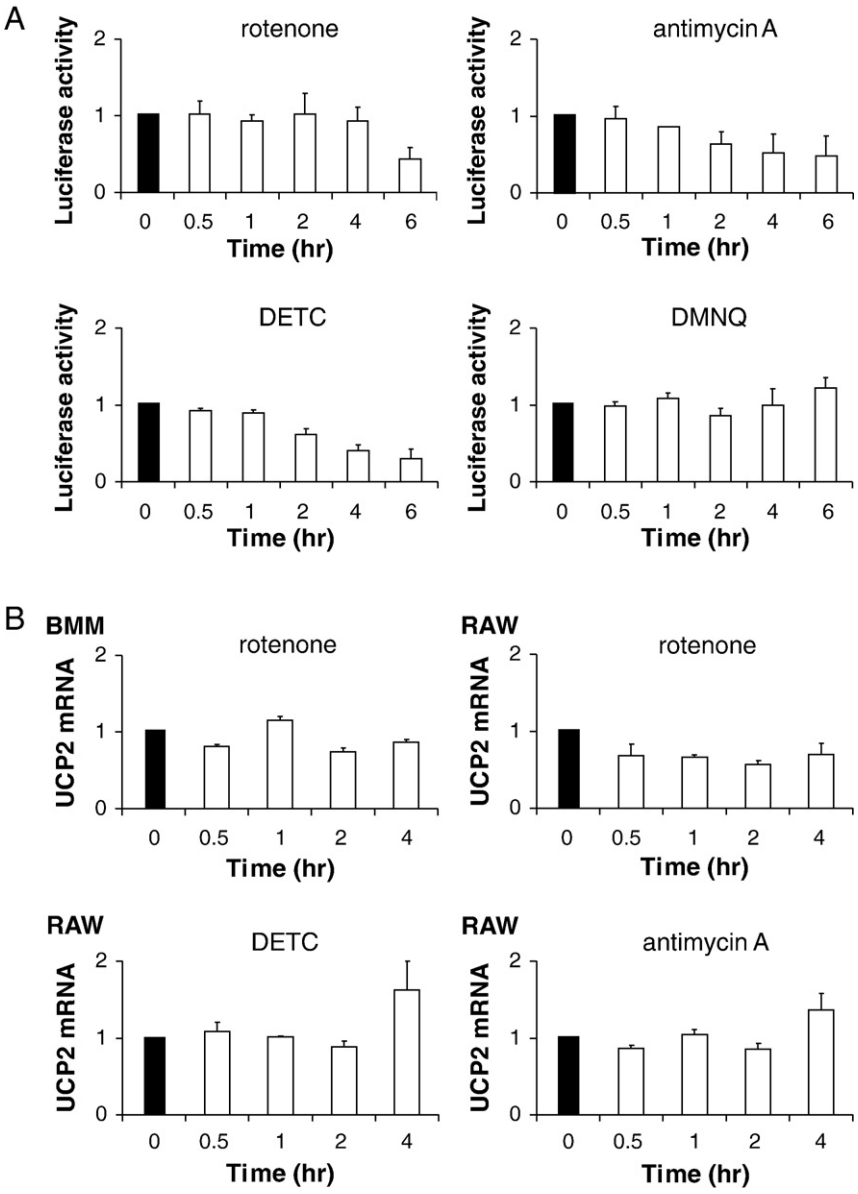

Fig. 4. Increased mitochondrial $O_2^{\bullet-}$ generation is not accompanied by increased *ucp2* promoter activity or UCP2 mRNA. (A) Reagents that increase mitochondrial $O_2^{\bullet-}$ production did not increase transcriptional activity of a reporter vector construct that incorporates the −2764 to +100 base pair promoter region of the *ucp2* gene, transiently transfected into $RAW_{264.7}$ cells. Results are shown as mean ± S.E.M for 3 or 4 independent experiments for each reagent, over 6 h of reagent exposure. Reagent concentrations were as for Fig. 1. Results are expressed as a ratio of luciferase activity in control cultures. (B) Rotenone failed to increase the abundance of UCP2 mRNA (top panels) over 4 h in either primary macrophages (left panel) or $RAW_{264.7}$ cells (right panel) respectively. DETC and antimycin A similarly failed to increase UCP2 mRNA of $RAW_{264.7}$ cells (bottom panels). UCP2 mRNA was estimated by RT-PCR. Results are shown as mean ± S.E.M for 3 independent experiments for each reagent and expressed as fold-increase over abundance in control cultures.

We therefore concluded that mitochondria-derived $O_2^{\bullet-}$ was not increasing UCP2 through increasing transcription or stability of UCP2 mRNA.

3.4. UCP2 accumulates in the mitochondrial inner membrane during increased $O_2^{\bullet-}$ generation

UCP2 is encoded in the nuclear genome. The protein is expressed in the inner mitochondrial membrane. In common with other members of its superfamily, UCP2 lacks a recognized mitochondrial targeting sequence. The pathways for introduction into the mitochondrial inner membrane and the pathways of degradation are largely unknown.

We therefore examined whether UCP2 protein stabilization was associated with enhanced accumulation in the inner mitochondrial membrane. $RAW_{264.7}$ cells were therefore treated with rotenone, antimycin A or DETC, and cells were collected for fractionation at 2h. Whole cell, mitochondria-enriched fraction, inner mitochondrial membrane (mitoplast) and intermembrane space fractions were prepared, as described in Methods. The recovery of mitochondrial protein was similar in control, rotenone-treated, antimycin A-treated and DETC-

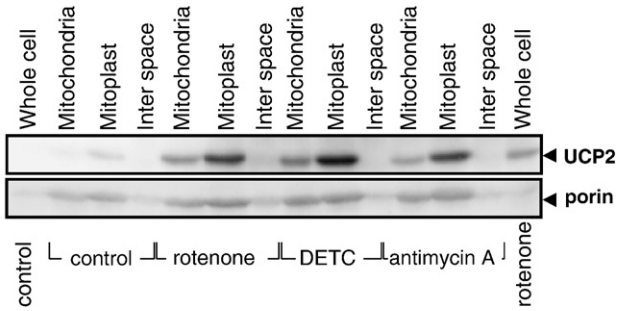

Fig. 5. UCP2 accumulates in the inner mitochondrial membrane (mitoplast fraction) of $RAW_{264.7}$ cells during periods of increased mitochondrial $O_2^{\bullet-}$ generation. Cells were treated for 2 h with rotenone (10 μM), antimycin A (10 μM) or DETC (0.3 mM). Results are representative of 7 repetitions with rotenone, all giving the same result. Antimycin A and DETC were tested once each. Equivalent amounts of protein (100 μg) were separated in each lane. The mitochondrial protein, porin was measured as a loading control to permit comparisons of whole mitochondrial and mitoplasts preparations under various conditions of stimulation. Extracts of untreated whole cells and rotenone-treated whole cells were run in the left-most and right-most lanes, respectively.

treated cells (mean recoveries of 102μg, 94μg, 126μg and 133μg per 10^7cells, respectively). In control cells, UCP2 was detected in preparations of mitochondria-enriched fraction and mitoplasts, and not in the intermembrane space, as expected (Fig. 5). Treatment with rotenone, antimycin A or DETC each greatly increased abundance in the mitochondria-enriched fraction and in the mitoplasts fraction, but not in the inter-membrane space (Fig. 5). These observations indicate that the increased expression of UCP2 that associates with increased mitochondrial $O_2^{\bullet-}$ generation arises from an accumulation of UCP2 in the inner mitochondrial membrane, where it can act to regulate $\Delta\psi_m$ and thereby regulate $O_2^{\bullet-}$ generation.

3.5. Induction of UCP2 during mitochondrial $O_2^{\bullet-}$ generation requires de-novo protein synthesis and is mediated though increased synthesis and possibly also protein stabilization

Previous experiments had shown that the increase in UCP2 protein occurred without an increase in UCP2 mRNA, implying an action on translation, recruitment to mitochondria or protein stability. In an attempt to distinguish enhanced protein synthesis from inhibited degradation, we measured the degradation rate of UCP2 in $RAW_{264.7}$ cells that had been exposed to rotenone, antimycin A or DETC for 2h before protein translation was halted by cycloheximide. UCP2 protein levels were measured by western analysis for a further 2h (Fig. 6A and B) Normally, UCP2 abundance in rotenone, antimycin A or DETC-exposed cultures continues to rise above control cultures during this time. However we observed that, when protein synthesis was blocked, UCP2 abundance in rotenone-, antimycin A-, and DETC-exposed cultures declined in parallel with controls preparations, indicating that UCP2 abundances did not continue to diverge in the absence of ongoing protein synthesis. Since rotenone, antimycin A and DETC do not increase UCP2 mRNA, this implies that they act, at least partly, by enhancing UCP2 mRNA translation.

The half life of UCP2 protein in the absence of the mitochondrial reagents was 73min ($n=9$ independent experiments). Strict comparisons of half life between $O_2^{\bullet-}$ enhanced and control conditions were inappropriate, because starting abundances of UCP2 differed and there was evidence for continuing UCP2 accumulation for up to 30min after addition of cycloheximide in rotenone and antimycin A-treated cultures. However, the crude exponential decay rates for UCP2 were non-significantly reduced in rotenone and DETC-treated cultures, but not in antimycin-A treated cultures, allowing the possibility that rotenone and DETC also affected protein stability. (Fig. 6A). UCP2 therefore accumulates during increased mitochondrial $O_2^{\bullet-}$ production because of increased translational efficiency and possibly also protein stabilization.

3.6. UCP2 protein accumulation is not through an action of mitochondrial $O_2^{\bullet-}$ on proteosomal degradation

Because the previous experiments allowed the possibility that protein stabilization contributed to UCP2 accumulation, we examined whether this reflected an action of mitochondria-derived $O_2^{\bullet-}$ on proteosomal degradation. However, blocking proteosomal function with MG 132 (10μM) did not lead to UCP2 accumulation and nor did it affect the accumulation stimulated by rotenone. This indicated that the association between mitochondrial $O_2^{\bullet-}$ production and UCP2 stabilization is not through any action on proteosomal degradation (results not shown).

3.7. UCP2 accumulation is not dependent on mitochondrial membrane potential

Insertion of the UCP2-related ANT1 protein into the inner mitochondrial membrane is potential-dependent [41]. Increased $\Delta\psi_m$ causes a non-linear increase in mitochondrial $O_2^{\bullet-}$ generation [42]. We therefore tested whether inner membrane UCP2 accumulation during mitochondrial $O_2^{\bullet-}$ generation depended on preservation of $\Delta\psi_m$.

$\Delta\psi_m$ was measured with the potential-dependent mitochondrial fluorophore, JC-1, as described in methods. Antimycin A decreased $\Delta\psi_m$ in $RAW_{264.7}$ cells as expected (Fig. 7). UCP2 is therefore not being recruited to the inner mitochondrial membrane, or being retained in it, because of any physicochemical process that depends on preserved or increased $\Delta\psi_m$.

Antimycin A inhibits complex III, which reduces $\Delta\psi_m$, but can also facilitate mitochondrial pore transition to reduce $\Delta\psi_m$ [43,44]. Cyclosporin A (1 μM), which blocks mitochondrial pore transition, did not prevent antimycin A-induced loss of $\Delta\psi_m$ (results not shown). This implies that antimycin A was largely reducing $\Delta\psi_m$ direct through complex III inhibition in these experiments.

4. Discussion

Under most circumstances, mitochondria are the most important source of reactive oxygen species intracellularly, both physiologically and in pathology. Single electron reduction of

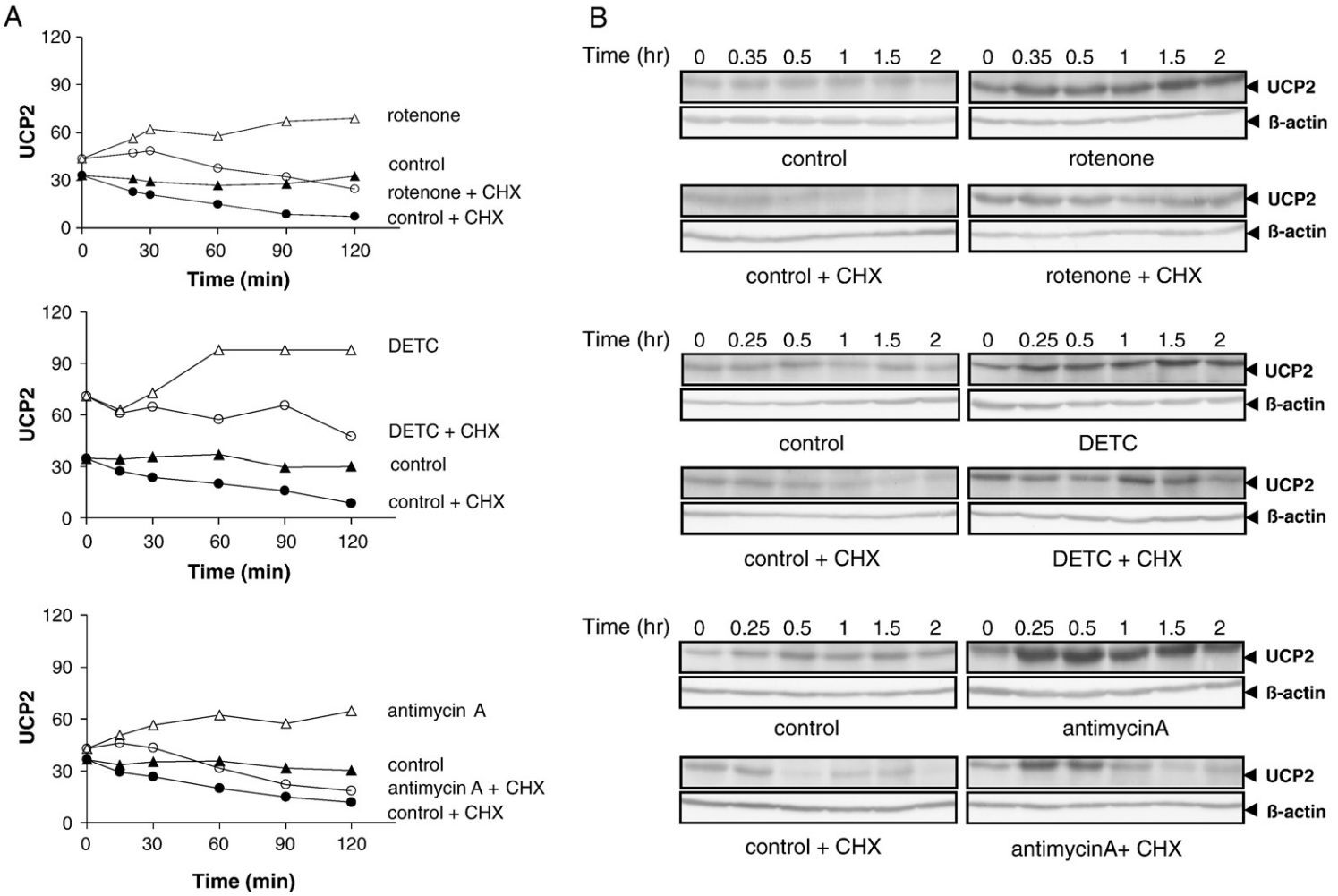

Fig. 6. UCP2 degradation rates are comparable in rotenone-exposed, antimycin A-exposed and unstimulated cultures. (A) When protein synthesis is inhibited with cycloheximide (CHX), UCP2 amounts decline at comparable rates in cells with normal (closed circles) and increased $O_2^{\bullet-}$ production (open circles), implying that the accumulation during oxidative stress is primarily due to enhanced UCP2 protein synthesis. Cells were exposed to rotenone, antimycin A or DETC as indicated, for 2 h before stopping protein synthesis. Graphs show mean scanned densities of UCP2 bands in western analyses of $RAW_{264.7}$ cells exposed to rotenone ($n=4$), antimycin A ($n=3$) and DETC ($n=3$), versus controls. Preliminary experiments with $RAW_{264.7}$ extracts showed that scanned density increased linearly with UCP2 protein loading (data not shown). UCP2 continues to accumulate when protein synthesis is not inhibited (open triangles). (B) Representative western analysis of UCP2 abundance in whole cell extracts of $RAW_{264.7}$ cells treated with rotenone, DETC or antimycin A, as described in panel A, with and without cycloheximide.

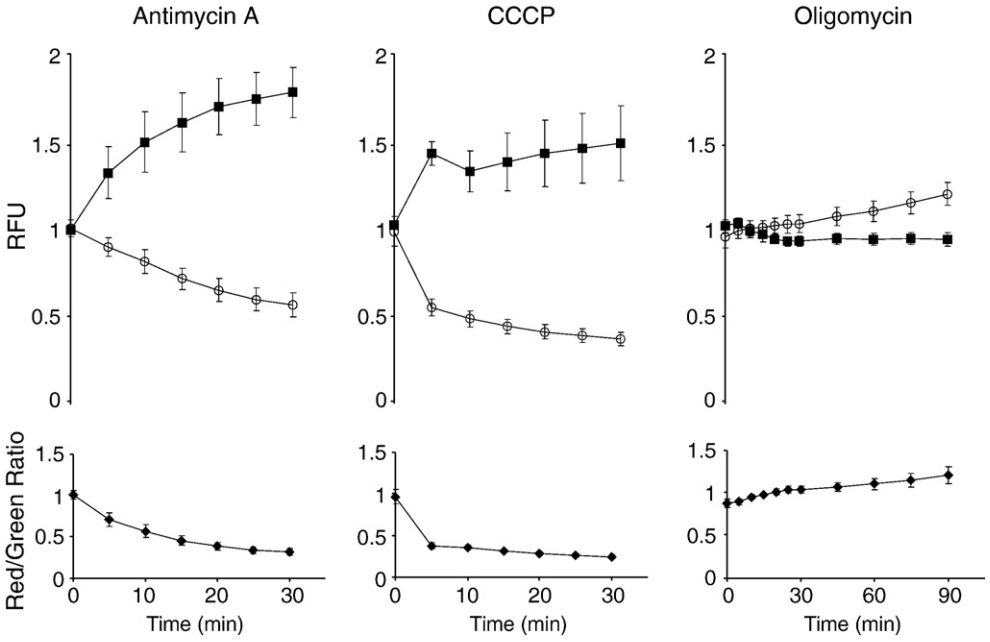

Fig. 7. UCP2 accumulation does not depend on preservation or increase of mitochondrial membrane potential. $\Delta\psi_m$ was measured with the potential-dependent mitochondrial flurophore, JC-1, after exposure to antimycin A (10 μM) or no treatment. Disappearance of red signal and replacement with green signal corresponds with loss of $\Delta\psi_m$-dependent localisation of the fluorophore in mitochondria. Results are shown as red fluorescence (○) and green fluorescence (■), normalised to contemporary controls (upper panels) and as ratios of normalised red signal to normalised green signal, over 30 or 90 m (lower panels). Antimycin A reduced $\Delta\psi_m$. Control experiments showed that the proton ionophore CCCP (10 μM) depolarised $\Delta\psi_m$ and the F_0F_1 ATPase inhibitor, oligomycin (1 μg/ml) hyperpolarised $\Delta\psi_m$, as expected. Results are means±S.E.M of 6 independent experiments for antimycin A and CCCP and 4 for oligomycin.

O_2 in mitochondria yields $O_2^{\bullet-}$, which then may dismute enzymatically to O_2 and H_2O_2. H_2O_2 may further reduce in the presence a transition metal, yielding highly reactive species that modify lipids, proteins and nucleic acids [11]. $O_2^{\bullet-}$ generated during activation of mitochondrial pathways of apoptosis interacts with Fe–sulfur centres in inner mitochondrial membrane respiratory complexes, disrupting electron flow and $\Delta\psi_m$ and leading ultimately to transition pore opening, cytochrome *C* release and activation of downstream intrinsic pathways of apoptosis [45]. Although excessive reactive oxygen species generation is destructive, there is some evidence for regulated production of $O_2^{\bullet-}$ for signaling purposes within the cell [46].

Mitochondrial production occurs during electron exchange between coenzyme Q and complexes I and III, at a rate that varies according to O_2 tension, redox status of the NAD(P)H pool [47] and $\Delta\psi_m$ [48,49]. Xenobiotics, such as the insecticide rotenone, that retard electron transfer between complex I or complex III and coenzyme Q also increase mitochondrial $O_2^{\bullet-}$ generation. Reactive oxygen species generated in mitochondria are removed by local superoxide dismutases and peroxidases and by reaction with low molecular weight reductants and sulfhydryl-containing protein reductants. Mitochondria contain both MnSOD and an isoform of Cu/Zn SOD. The effectiveness of Cu/Zn SOD in clearing $O_2^{\bullet-}$ is revealed by the accumulation of $O_2^{\bullet-}$ that occurs when it is blocked in mitochondria and cytosol with DETC (Fig. 1B).

Mechanisms for removal of mitochondrial reactive oxygen species are thus well described. Additionally, uncoupling proteins lower $\Delta\psi_m$ and thereby limit ROS production [8,42]. UCP2 mRNA is widely distributed in tissue, but mostly without detectable protein expression, or with low-level constitutive expression [7]. Abundant constitutive expression of inner membrane uncoupling proteins, outside the thermoregulatory function of UCP1 in brown adipose tissue, would be energetically wasteful. However, regulated expression of UCP2 would provide a mechanism for adjusting mitochondrial ROS production in cell types, such as macrophages, that must function in widely varying tissue environments. UCP2 protein is relatively abundant in macrophage lineage cells [7]. A role in regulating macrophage ROS production has been demonstrated [8].

In these studies, we observed that UCP2 has a short half life in macrophages of around 1 h. Similarly rapid elimination has been documented in mammalian cells overexpressing UCP2 and in yeast cells engineered to express the protein [50]. UCP2 is regulated in macrophages, increasing rapidly in response to a range of stimuli that increased mitochondrial $O_2^{\bullet-}$ generation. UCP2 is nuclear encoded and synthesized on cytosolic ribosomes before import into mitochondria [51,52]. Transcriptional regulation of *ucp2* has been described for PPAR ligands [53,54] and lipopolysaccharide [23], but we did not find evidence for increased *ucp2* gene transcription in response to mitochondrial $O_2^{\bullet-}$ generation. mRNA stabilization was also excluded as a explanation by observing that UCP2 mRNA abundance did not increase when UCP2 protein increased.

UCP2 protein abundance poorly reflects mRNA abundance in tissue, implying important regulatory functions in translation or protein stability [6]. There is evidence for regulation of translation through regions in the untranslated exon 2, me-

diating response to lipopolysaccharide [6,23]. Additionally, heterogenous nuclear ribonucleoprotein K (hnRNPK), which has activities in translational regulation, has been shown to bind to sequences in UCP2 mRNA 3′ UTR in yeast 3-hybrid screening. The complex is found in association with both polysomes and mitochondria in cultured rat hepatoma cells [35]. Insulin induction of UCP2 protein in hepatoma cells is enhanced by hnRNPK expression [35], implying that it is translationally-mediated. Our observation, that rotenone failed to further enhance UCP2 abundance after protein synthesis was interrupted with cycloheximide, also implies an action of translation.

Although these experiments indicated that regulation by reactive oxygen species was primarily translational, there were non-significant reductions in degradation rate in the presence of DETC and rotenone, allowing the possibility that UCP2 protein was also stabilized in the inner mitochondrial membrane during reactive oxygen species generation. Experiments with the proteosomal inhibitor MG 132 showed that UCP2 was not a substrate for the proteosomal pathway, excluding this as a possible pathway of regulation. The pathways of UCP2 degradation in mitochondria are unknown. The broad specificity mitochondrial AAA proteases located on the inner mitochondrial membrane, and active either on the intermembrane space surface (i-AAA) or the matrix surface (m-AAA), are potential candidates [55,56], though they have not been found to be active against UCP2 overexpressed in yeast [50].

Cell fractionation showed that the newly synthesized UCP2 primarily appeared in a fraction that was enriched for mitochondria, though may have contained contributions from other organelles, such as endoplasmic reticulum. UCP2 could potentially accumulate in mitochondrial through more efficient recruitment into the organelle and away from cytosolic pathways of degradation. The mechanism of UCP2 recruitment to the inner mitochondrial membrane has not been specifically studied. UCP2 does not have a known targeting sequence. The related ANT1 protein is recruited to the inner mitochondrial membrane through a sequence of interactions with TIM (Transporter of Inner Membrane) proteins, firstly with a complex of Tim9p and Tim10p proteins in the intermembrane space and then with Tim proteins already resident in the inner mitochondrial membrane. There is evidence that redox status influences both stages [41,57] and that $\Delta\psi_m$ regulates retention in the inner mitochondrial membrane [52,58]. We can conclude that recruitment of additional UCP2 to the inner mitochondrial membrane does not require increased $\Delta\psi_m$, because it occurs with antimycin A, which reduces $\Delta\psi_m$.

In these experiments, induction of UCP2 correlated strictly with increased mitochondrial $O_2^{\bullet-}$ production. We did not prove that other cellular source of $O_2^{\bullet-}$ could not induce UCP2, but observed that neither $O_2^{\bullet-}$ generated at the cell surface NAD(P)H oxidase nor $O_2^{\bullet-}$ generated by redox-cycling of DMNQ in cytosol and extracellularly [40] induced UCP2. This may reflect the short diffusion distance of reactive $O_2^{\bullet-}$ or the presence of cytosolic Cu/Zn SOD. Our experiments do not reveal how mitochondrial UCP2 regulation is isolated from changes in extra-mitochondrial ROS levels. Isolation would prevent incidental changes in extra-mitochondrial ROS levels from compromising the efficiency of mitochondrial energy metabolism by modifying UCP2 abundance.

These findings extend our understanding of the homeostatic function of UCP2 in regulating mitochondrial reactive oxygen production by identifying the afferent limb of a feedback loop that senses mitochondrial reactive oxygen production, and increases inner mitochondrial membrane expression of UCP2. UCP2 diminishes mitochondrial ROS production in macrophages [8,23].

Acknowledgment

This work was supported by a Goatcher Clinical Research Unit Scholarship awarded to Tindaro Giardina.

References

[1] S. Krauss, C.Y. Zhang, B.B. Lowell, The mitochondrial uncoupling-protein homologues, Nat. Rev., Mol. Cell. Biol. 6 (2005) 248–261.
[2] D. Ricquier, J.C. Kader, Mitochondrial protein alteration in active brown fat: a sodium dodecyl sulfate-polyacrylamide gel electrophoretic study, Biochem. Biophys. Res. Commun. 73 (1976) 577–583.
[3] D.G. Nicholls, A history of UCP1, Biochem. Soc. Trans. 29 (2001) 751–755.
[4] D.G. Nicholls, R.M. Locke, Thermogenic mechanisms in brown fat, Physiol. Rev. 64 (1984) 1–64.
[5] J. Mozo, Y. Emre, F. Bouillaud, D. Ricquier, F. Criscuolo, Thermoregulation: what role for UCPs in mammals and birds? Biosci. Rep. 25 (2005) 227–249.
[6] C. Pecqueur, M.C. Alves-Guerra, C. Gelly, C. Levi-Meyrueis, E. Couplan, S. Collins, D. Ricquier, F. Bouillaud, B. Miroux, Uncoupling protein 2, in vivo distribution, induction upon oxidative stress, and evidence for translational regulation, J. Biol. Chem. 276 (2001) 8705–8712.
[7] G. Mattiasson, P.G. Sullivan, The emerging functions of UCP2 in health, disease, and therapeutics, Antioxid. Redox Signal. 8 (2006) 1–38.
[8] D. Arsenijevic, H. Onuma, C. Pecqueur, S. Raimbault, B.S. Manning, B. Miroux, E. Couplan, M.C. Alves-Guerra, M. Goubern, R. Surwit, F. Bouillaud, D. Richard, S. Collins, D. Ricquier, Disruption of the uncoupling protein-2 gene in mice reveals a role in immunity and reactive oxygen species production, Nat. Genet. 26 (2000) 435–439.
[9] J.A. Stuart, J.A. Harper, K.M. Brindle, M.B. Jekabsons, M.D. Brand, Physiological levels of mammalian uncoupling protein 2 do not uncouple yeast mitochondria, J. Biol. Chem. 276 (2001) 18633–18639.
[10] S. Rousset, M.C. Alves-Guerra, J. Mozo, B. Miroux, A.M. Cassard-Doulcier, F. Bouillaud, D. Ricquier, The biology of mitochondrial uncoupling proteins, Diabetes 53 (Suppl 1) (2004) S130–S135.
[11] B. Halliwell, J.M.C. Gutteridge, Free Radicals in Biology and Medicine, 4th edition. Oxford University Press, Oxford, 2007.
[12] S.S. Korshunov, V.P. Skulachev, A.A. Starkov, High protonic potential actuates a mechanism of production of reactive oxygen species in mitochondria, FEBS Lett. 416 (1997) 15–18.
[13] S.S. Liu, Generating, partitioning, targeting and functioning of superoxide in mitochondria, Biosci. Rep. 17 (1997) 259–272.
[14] E. Cadenas, K.J. Davies, Mitochondrial free radical generation, oxidative stress, and aging, Free Radic. Biol. Med. 29 (2000) 222–230.
[15] M.D. Brand, C. Affourtit, T.C. Esteves, K. Green, A.J. Lambert, S. Miwa, J.L. Pakay, N. Parker, Mitochondrial superoxide: production, biological effects, and activation of uncoupling proteins, Free Radic. Biol. Med. 37 (2004) 755–767.
[16] T.V. Votyakova, I.J. Reynolds, DeltaPsi(m)-Dependent and -independent production of reactive oxygen species by rat brain mitochondria, J. Neurochem. 79 (2001) 266–277.
[17] S.S. Liu, Cooperation of a “reactive oxygen cycle” with the Q cycle and the proton cycle in the respiratory chain—superoxide generating and

cycling mechanisms in mitochondria, J. Bioenerg. Biomembr. 31 (1999) 367–376.
[18] K.S. Echtay, D. Roussel, J. St-Pierre, M.B. Jekabsons, S. Cadenas, J.A. Stuart, J.A. Harper, S.J. Roebuck, A. Morrison, S. Pickering, J.C. Clapham, M.D. Brand, Superoxide activates mitochondrial uncoupling proteins, Nature 415 (2002) 96–99.
[19] S. Miwa, J. St-Pierre, L. Partridge, M.D. Brand, Superoxide and hydrogen peroxide production by *Drosophila* mitochondria, Free Radic. Biol. Med. 35 (2003) 938–948.
[20] A. Negre-Salvayre, C. Hirtz, G. Carrera, R. Cazenave, M. Troly, R. Salvayre, L. Penicaud, L. Casteilla, A role for uncoupling protein-2 as a regulator of mitochondrial hydrogen peroxide generation, Faseb J. 11 (1997) 809–815.
[21] N. Produit-Zengaffinen, N. Davis-Lameloise, H. Perreten, D. Becard, A. Gjinovci, P.A. Keller, C.B. Wollheim, P. Herrera, P. Muzzin, F. Assimacopoulos-Jeannet, Increasing uncoupling protein-2 in pancreatic beta cells does not alter glucose-induced insulin secretion but decreases production of reactive oxygen species, Diabetologia 50 (2007) 84–93.
[22] Y. Teshima, M. Akao, S.P. Jones, E. Marban, Uncoupling protein-2 overexpression inhibits mitochondrial death pathway in cardiomyocytes, Circ. Res. 93 (2003) 192–200.
[23] T. Kizaki, K. Suzuki, Y. Hitomi, N. Taniguchi, D. Saitoh, K. Watanabe, K. Onoe, N.K. Day, R.A. Good, H. Ohno, Uncoupling protein 2 plays an important role in nitric oxide production of lipopolysaccharide-stimulated macrophages, Proc. Natl. Acad. Sci. U. S. A. 99 (2002) 9392–9397.
[24] J.S. Lewis, J.A. Lee, J.C. Underwood, A.L. Harris, C.E. Lewis, Macrophage responses to hypoxia: relevance to disease mechanisms, J. Leukoc. Biol. 66 (1999) 889–900.
[25] C.E. Lewis, J.W. Pollard, Distinct role of macrophages in different tumor microenvironments, Cancer Res. 66 (2006) 605–612.
[26] C. Murdoch, M. Muthana, C.E. Lewis, Hypoxia regulates macrophage functions in inflammation, J. Immunol. 175 (2005) 6257–6263.
[27] M.S. Wolin, M. Ahmad, S.A. Gupte, Oxidant and redox signaling in vascular oxygen sensing mechanisms: basic concepts, current controversies, and potential importance of cytosolic NADPH, Am. J. Physiol. Lung Cell. Mol. Physiol. 289 (2005) L159–L173.
[28] A.S. Marsin, C. Bouzin, L. Bertrand, L. Hue, The stimulation of glycolysis by hypoxia in activated monocytes is mediated by AMP-activated protein kinase and inducible 6-phosphofructo-2-kinase, J. Biol. Chem. 277 (2002) 30778–30783.
[29] H.J. Forman, M. Torres, Redox signaling in macrophages, Mol. Aspects Med. 22 (2001) 189–216.
[30] M.P. Murphy, K.S. Echtay, F.H. Blaikie, J. Asin-Cayuela, H.M. Cocheme, K. Green, J.A. Buckingham, E.R. Taylor, F. Hurrell, G. Hughes, S. Miwa, C.E. Cooper, D.A. Svistunenko, R.A. Smith, M.D. Brand, Superoxide activates uncoupling proteins by generating carbon-centered radicals and initiating lipid peroxidation: studies using a mitochondria-targeted spin trap derived from alpha-phenyl-*N*-tert-butylnitrone, J. Biol. Chem. 278 (2003) 48534–48545.
[31] K.S. Echtay, T.C. Esteves, J.L. Pakay, M.B. Jekabsons, A.J. Lambert, M. Portero-Otin, R. Pamplona, A.J. Vidal-Puig, S. Wang, S.J. Roebuck, M.D. Brand, A signalling role for 4-hydroxy-2-nonenal in regulation of mitochondrial uncoupling, Embo J. 22 (2003) 4103–4110.
[32] C. Hurtaud, C. Gelly, F. Bouillaud, C. Levi-Meyrueis, Translation control of UCP2 synthesis by the upstream open reading frame, Cell Mol. Life Sci. 63 (2006) 1780–1789.
[33] J. Nedergaard, B. Cannon, The 'novel' 'uncoupling' proteins UCP2 and UCP3: what do they really do? Pros and cons for suggested functions, Exp. Physiol. 88 (2003) 65–84.
[34] K.H. Yip, M.H. Zheng, J.H. Steer, T.M. Giardina, R. Han, S.Z. Lo, A.J. Bakker, A.I. Cassady, D.A. Joyce, J. Xu, Thapsigargin modulates osteoclastogenesis through the regulation of RANKL-induced signaling pathways and reactive oxygen species production, J. Bone Miner. Res. 20 (2005) 1462–1471.
[35] J. Ostrowski, K. Klimek-Tomczak, L.S. Wyrwicz, M. Mikula, D.S. Schullery, K. Bomsztyk, Heterogeneous nuclear ribonucleoprotein K enhances insulin-induced expression of mitochondrial UCP2 protein, J. Biol. Chem. 279 (2004) 54599–54609.
[36] P. Klement, L.G. Nijtmans, C. Van den Bogert, J. Houstek, Analysis of oxidative phosphorylation complexes in cultured human fibroblasts and amniocytes by blue-native-electrophoresis using mitoplasts isolated with the help of digitonin, Anal. Biochem. 231 (1995) 218–224.
[37] J.H. Steer, K.M. Kroeger, L.J. Abraham, D.A. Joyce, Glucocorticoids suppress tumor necrosis factor-alpha expression by human monocytic THP-1 cells by suppressing transactivation through adjacent NF-kB and c-Jun-activating transcription factor-2 binding sites in the promoter, J. Biol. Chem 275 (2000) 18432–18440.
[38] M. Degli Esposti, Measuring mitochondrial reactive oxygen species, Methods 26 (2002) 335–340.
[39] M.M. Tarpey, D.A. Wink, M.B. Grisham, Methods for detection of reactive metabolites of oxygen and nitrogen: in vitro and in vivo considerations, Am. J. Physiol. Regul. Integr. Comp. Physiol. 286 (2004) R431–R444.
[40] N. Watanabe, H.J. Forman, Autoxidation of extracellular hydroquinones is a causative event for the cytotoxicity of menadione and DMNQ in A549-S cells, Arch. Biochem. Biophys. 411 (2003) 145–157.
[41] S.P. Curran, D. Leuenberger, E.P. Leverich, D.K. Hwang, K.N. Beverly, C.M. Koehler, The role of Hot13p and redox chemistry in the mitochondrial TIM22 import pathway, J. Biol. Chem. 279 (2004) 43744–43751.
[42] B. Kadenbach, Intrinsic and extrinsic uncoupling of oxidative phosphorylation, Biochim. Biophys. Acta 1604 (2003) 77–94.
[43] M.K. Manion, J.W. O'Neill, C.D. Giedt, K.M. Kim, K.Y. Zhang, D.M. Hockenbery, Bcl-XL mutations suppress cellular sensitivity to antimycin A, J. Biol. Chem. 279 (2004) 2159–2165.
[44] S.P. Tzung, K.M. Kim, G. Basanez, C.D. Giedt, J. Simon, J. Zimmerberg, K.Y. Zhang, D.M. Hockenbery, Antimycin A mimics a cell-death-inducing Bcl-2 homology domain 3, Nat. Cell Biol. 3 (2001) 183–191.
[45] J.D. Ly, D.R. Grubb, A. Lawen, The mitochondrial membrane potential (deltapsi(m)) in apoptosis; an update, Apoptosis 8 (2003) 115–128.
[46] S. Pervaiz, M.V. Clement, A permissive apoptotic environment: function of a decrease in intracellular superoxide anion and cytosolic acidification, Biochem. Biophys. Res. Commun. 290 (2002) 1145–1150.
[47] G. Lenaz, The mitochondrial production of reactive oxygen species: mechanisms and implications in human pathology, IUBMB Life 52 (2001) 159–164.
[48] J.F. Turrens, Mitochondrial formation of reactive oxygen species, J. Physiol. 552 (2003) 335–344.
[49] J.F. Turrens, B.A. Freeman, J.G. Levitt, J.D. Crapo, The effect of hyperoxia on superoxide production by lung submitochondrial particles, Arch. Biochem. Biophys. 217 (1982) 401–410.
[50] S. Rousset, J. Mozo, G. Dujardin, Y. Emre, S. Masscheleyn, D. Ricquier, A.M. Cassard-Doulcier, UCP2 is a mitochondrial transporter with an unusual very short half-life, FEBS Lett. 581 (2007) 479–482.
[51] J.M. Herrmann, K. Hell, Chopped, trapped or tacked—Protein translocation into the IMS of mitochondria, Trends Biochem. Sci. 30 (2005) 205–211.
[52] C.M. Koehler, New developments in mitochondrial assembly, Annu. Rev. Cell Dev. Biol. 20 (2004) 309–335.
[53] A.V. Medvedev, J. Robidoux, X. Bai, W. Cao, L.M. Floering, K.W. Daniel, S. Collins, Regulation of the uncoupling protein-2 gene in INS-1 beta-cells by oleic acid, J. Biol. Chem. 277 (2002) 42639–42644.
[54] M.P. Thompson, D. Kim, Links between fatty acids and expression of UCP2 and UCP3 mRNAs, FEBS Lett. 568 (2004) 4–9.
[55] D.A. Bota, K.J. Davies, Protein degradation in mitochondria: implications for oxidative stress, aging and disease: a novel etiological classification of mitochondrial proteolytic disorders, Mitochondrion 1 (2001) 33–49.
[56] I. Arnold, T. Langer, Membrane protein degradation by AAA proteases in mitochondria, Biochim. Biophys. Acta 1592 (2002) 89–96.
[57] C.M. Koehler, K.N. Beverly, E.P. Leverich, Redox pathways of the mitochondrion, Antioxid. Redox Signal. 8 (2006) 813–822.
[58] A.E. Frazier, A. Chacinska, K.N. Truscott, B. Guiard, N. Pfanner, P. Rehling, Mitochondria use different mechanisms for transport of multispanning membrane proteins through the intermembrane space, Mol. Cell. Biol. 23 (2003) 7818–7828.